39. PV-Symposium 2024

Conference paper

https://doi.org/10.52825/pv-symposium.v1i.1011

Published: 05 Aug. 2024

Evaluation of Light-Induced Electroluminescence in Photovoltaic Field Applications

Marc Köntges[1], Michael Siebert[1], Andreas Fladung[2], and Jan Schlipf[2]

[1] Institut für Solarenergieforschung GmbH (ISFH), Germany

[2] Aerial PV Inspection GmbH, Germany

Abstract. We present a performance analysis of the new measurement method Light-Induced Electroluminescence (LIEL) in a PV system. The LIEL method is applied to photovoltaic (PV) modules consisting of two PV module halves which are internally connected in parallel. Today's main stream half-cell modules are constructed this way. To measure the electroluminescence of one half of the module, the other half is illuminated by an LED array. Our LIEL prototype system is a hood-based setup. It is equipped on one half with a LED array that is separated by a wall from the other half. This other half is observed by an InGaAs camera. We measure the impact of a LIEL hood misalignment to the electroluminescence intensity, the influence of the PV generator working point to the electroluminescence intensity and determine the measurement speed under realistic conditions. We show that the experimentally realized LIEL hood alignment to the PV modules is in 97.7% of the cases sufficient for acquiring high quality EL images. The LIEL system work with a switched off and on inverter. Under inverter on working condition the luminescence intensity is a function of the intensity of the sun. The effect of hood alignment and sun intensity on the luminescence intensity is successfully reproduced by an analogue electronic circuit simulation using LT Spice. The maximum measuring speed of a full module is in this study 12 s including the time for movement and alignment of the measurement hood from PV module to PV module.

Keywords: Electroluminescence, PV Module Characterisation, PV Module Failure

1. Introduction

Solar parks are usually checked for defects in the solar field using infrared images taken by drones [1]. This monitoring method is particularly simple and time-efficient. Unfortunately, not all faults in the solar modules can be detected using this method and the measurement can only be carried out during the day when there is intense, stable sunlight higher than 600 W/m² [1].

Electroluminescence (EL) measurements reveal much more defect types in the photovoltaic (PV)-modules but need and electrical connection to the measurement system and it is done during night time [1]. However, the electrical connection of the EL measurement equipment is time consuming, a trained electrician is needed and it adds the risk of breaking contacts or wrong reassembly afterwards. Therefore, many attempts are made to increase the applicability to measure electroluminescence or photoluminescence (PL) [2, 3]. There are new techniques to measure photoluminescence without disconnecting the PV modules from the inverter by using the inverter global maximum power point (mpp) search as switch between weakly and intense luminescing operation points enabling to extract non-wanted image information from the PL-image [4]. As the global mpp search happens about all 6 min, the method is slow. To

increase the speed and the scope of application Benatto et al. present a drone base daylight EL/PL measurement method [5]. They use an InGaAs camera with an EL filter and a dark frame subtraction applied together with an image motion compensation technique, to generate EL images during daylight. However, for this application the PV-generator must be rewired.

***Figure 1**. Application of the LIEL measuring hood in the solar park.*

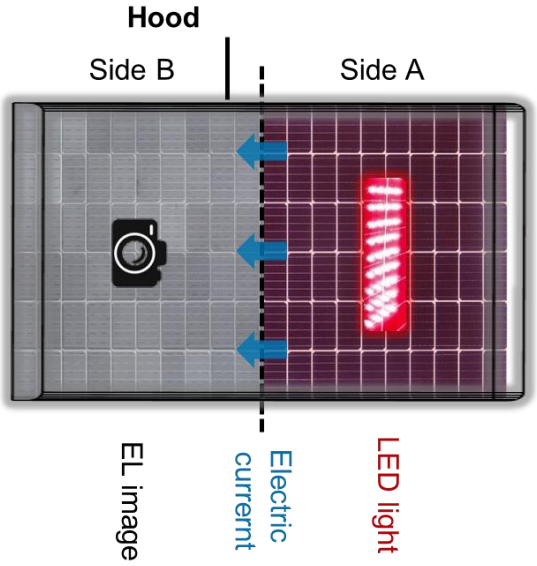

***Figure 2**. Scheme of the measurement method, with the same orientation as in Fig.1.*

In this paper we present for the first time the application of the Light-Induced electroluminescence (LIEL) technique in the field, see Fig. 1. The theoretical principles of the measurement method and evaluations on a lab setup and a sun driven outdoor setup have already been published by Köntges et al. [6]. In that publication the effect of inhomogeneous light source and various PV module defect types on the electroluminescence pattern has been analysed. This new technique can be applied to PV modules with parallel interconnected cell strings in one module. Nearly all current module types on the mainstream market are based on half-cut cells being interconnected in a series-parallel interconnection and therefore fulfil this condition. The new LIEL method uses a LED flash light pulse on the module halve A to drive an electric current through the other parallel connected module halve B. This excites the part B to electroluminescence. See Fig. 2 for the definition of the PV module sides A and B. In this publication, we examine how the method performs under real conditions in a PV park. In Fig. 3 an example defective PV module is shown measured with this new technique in the field.

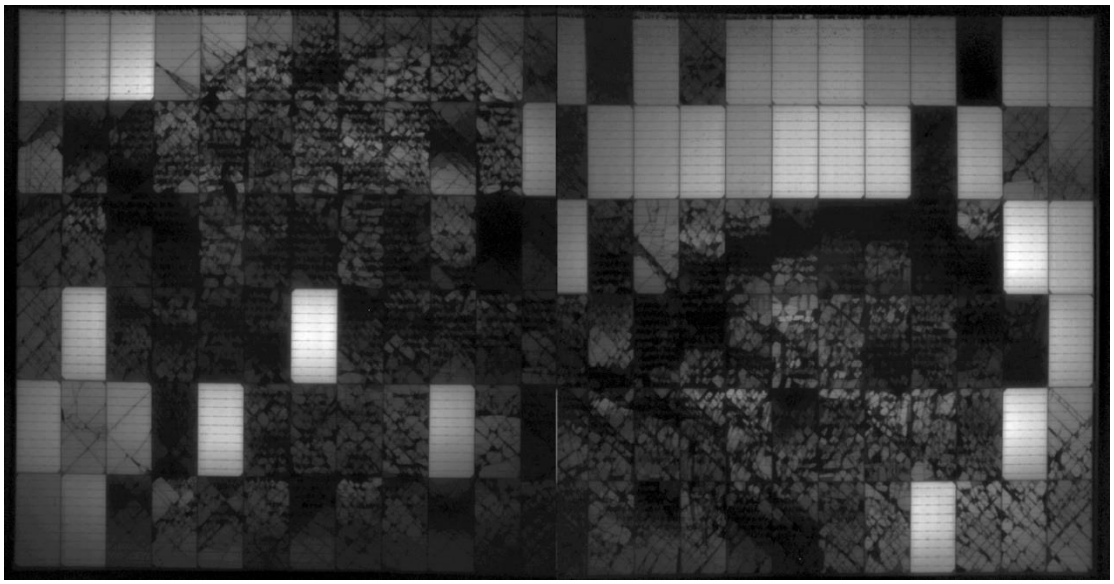

***Figure 3**. LIEL image of a defective solar module with the dimensions 2279 mm x 1134 mm. The image was composed from two LIEL images. The lens distortion was removed and the image intensity was adjusted for a suitable visualisation. At the upper edge of the image some bristles of the brushes used to prevent external light reaching into the measurement hood can be seen.*

2. Method

2.1 Experimental

A 16 kg test cover, see Fig. 4, has been developed that can be variably adapted to different module sizes. The measuring device is powered by two lightweight batteries that are carried along and provide energy for at least 400 PV module measurements. As shown in Fig. 4a, the test cover consists of an illumination unit on one side, which illuminates the half A of the solar module with 576 LEDs with an irradiation power of 2.25 W each (centre wave length at 850 nm). The light source is designed to be so flexible that it can be adapted to various of today's module sizes (from 1.6 m x 0.95 m to 2.4 m x 1.3 m). As the LIEL measurement technology requires a high light output, the LED light source is designed in such a way that it generates approx. 0.7 times the I_{sc} current in a half-cell module when illuminating only one half of the module. The LED intensity is fixed. An InGaAs camera with a resolution of 1024 pixels x 1280 pixels is used to record images on the electroluminescent side B of the solar module. Both parts of the measuring hood are separated from each other by a separator wall so that no excitation light from the LEDs can reach the camera side. Light components that nevertheless reach the camera side due to light scattering within the module glass are filtered out by a narrow band-pass filter BP1150 with a centre wave length of 1150 nm and a half-width of 50 nm. Fig. 4 shows how this filter correspond to other light sources in the field (Sun spectrum, excitation LEDs and EL-signal). In the practical application the LEDs can be pulsed for 50 ms up to 200 ms. Within this time duration the InGaAs camera takes an image of the luminescence part of the module. To extract the effect of stray light from below the PV module bank or not perfectly closed hood, a dark frame image is taken when the LED light is off. For the final image the dark frame image is subtracted from the regular electroluminescence image.

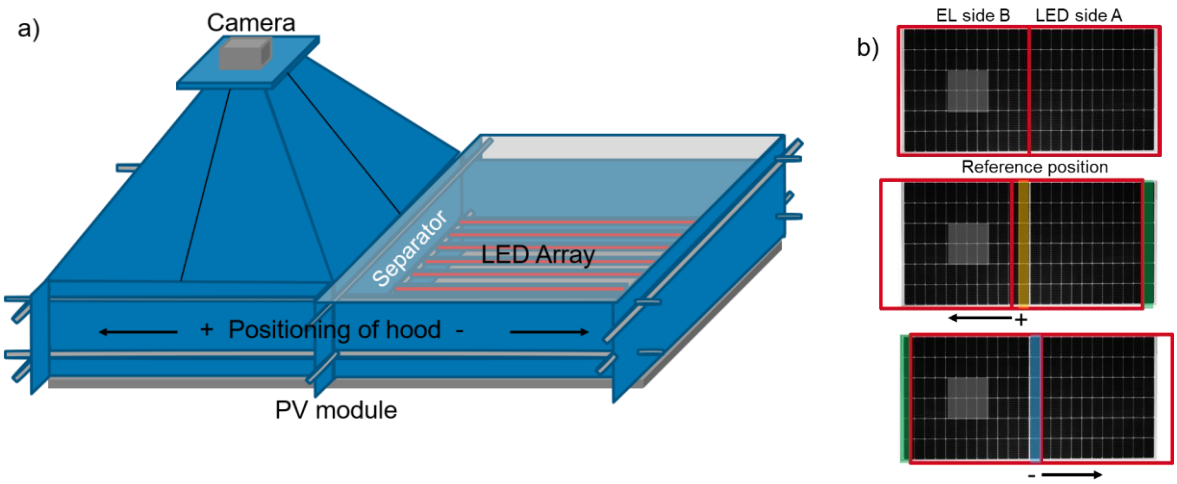

***Figure 4**. Left (a): Sketch of the measuring tool with definition of the misalignment directions. Right (b): Effect of moving the LIEL cover to plus or minus direction relative to the reference position. Red frame indicates the edges and the separator of the LIEL system. Grey area: region where the EL intensity is evaluated, orange area: luminescence cells receive unwanted LED light, green area: cells receive sun-irradiation or no irradiation in the night, blue area: cells receive no LED irradiation.*

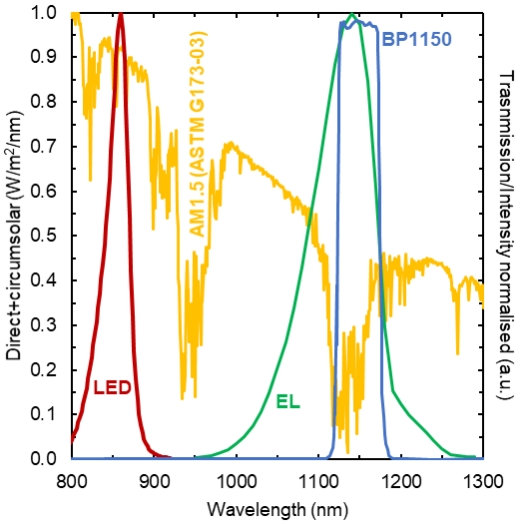

***Figure 5**. Spectral comparison of all light sources in the LIEL setup with the camera filter BP1150 transmission. Mainly the EL signal with some stray light from the module rear may reach the camera trough the BP1150 filter.*

During our tests, the incident light intensity on module level is measured with a pyranometer each 60 seconds. We measured intensities from 0 W/m² in the night up to 830 W/m² at high noon.

LIEL images of module strings with connected inverter (MPP images) and with disconnected inverters (V_{OC} images) were recorded and compared with each other. For the comparison the mean EL intensity of 8 middle cells in the middle substring of the modules is used. The electroluminescence area used for this averaging is marked in Fig. 4b by a grey coloured rectangle on the PV module. The recorded EI intensity is an indicator for the operation point of the investigated cells and the quality of the acquisition.

In order to check the robustness of the measuring unit in the free field, LIEL recordings were made with the measuring hood intentionally positioned incorrectly. The influence of the

incorrect positioning on the EL intensity is analysed with the modules disconnected from the inverter (V_{OC}). Measurements are carried out on the western half of the module and the eastern half of the module. The intentional misalignment is carried out along the longitudinal axis of a module and specified in mm from the optimum position. Positive values indicate a shift of the camera position towards the edge of the module, negative values indicate a shift towards the centre of the module, see Fig. 4a. In the case of exact positioning, the partition wall between the LED array and the chamber area is positioned exactly on the middle cross-connection of the half-cell module. The misalignment is measured by counting the pixel deviation of an image against an optimal reference position. The pixel length is calibrated by counting the pixel of a solar cell in the image. One half-cell has the dimension of 182 mm x 91 mm. For comparison to the simulations the misalignment is expressed as a misalignment in fractions of a half-cell [0..1]. The misalignment can cause a shade on a cell (blue area), non-intended LED illumination (orange area) or non-intended sun irradiation (green area) as illustrated in Fig. 4b.

Furthermore, the statistics of incorrect positioning was analysed on 261 measurements carried out in the park. This allows to assess how often and to what extent images were influenced by incorrect positioning.

The measured modules in the field were 2279 mm long, 1134 mm wide, use 144 M10 half-cells with a width of 182 mm and a length of 91 mm. The modules consist of 6 substrings each with 24 cells in series. There are always two substrings in parallel per module. Three of these parallel connections are in series. The main electrical module data is presented in Tab. 1.

The PV system studied here consists of 27 PV modules in series with two of these series connected module strings in parallel on one MPP tracked inverter input.

Table 1. *PV module parameter of the tested PV system and used simulation parameter.*

Parameter	**Value Data sheet**	**Simulation**
Maximum Power at STC P_{mpp}	545 W	545.5 W
Optimum Operation Voltage V_{mpp}	41.8 V	41.14 V
Optimum Operation Current I_{mpp}	13.02 A	13.25 A
Open Circuit Voltage V_{oc}	49.69 V	49.21 V
Short Circuit Current I_{sc}	13.96 A	13.98 A
Cell area A_{cell}	M10 half-cell ~16500 mm²	16500 mm²
Short circuit density j_{sc}		42.35 mA/cm²
Saturation current diode 1 J_{01}		$14*10^{-14}$ A/cm²
Saturation current diode 2 J_{02}		$1*10^{-11}$ A/cm²
Ideality factor diode 1		1
Ideality factor diode 2		2
Series resistance R_s		0.77 Ohm cm²
Parallel resistance R_p		2 kOhm cm²

As the LED light sources are arranged in lines without providing any compensation to edge effects it is expected that the LED light on the PV module cells is inhomogeneous. Therefore, we measured the light homogeneity of the setup in one corner with a short circuit measurement of a laminated half-cell with a cell size of 165 mm x 82 mm. Figure 6 shows the results. We expect that the results are symmetric as the LIEL setup is symmetric. Within one substring we can expect that the string edge cells receive 80% of the light intensity of the cells in the middle of the string.

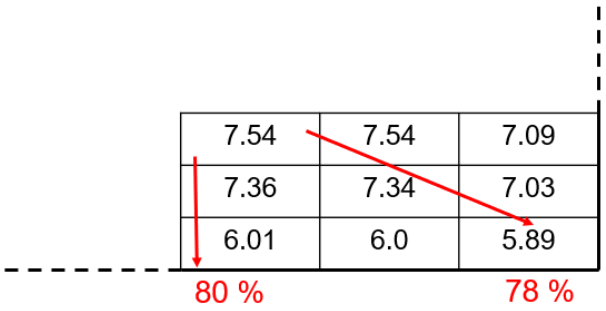

***Figure 6**. Measured light homogeneity of the LED light source in the LIEL cover at one edge. The values are given in Ampere of a test solar cell.*

2.2 Simulations

We simulate the influence of LIEL hood misalignment at V_{OC} working point on the LIEL luminescence intensity by an analogue electronic circuit simulation using LT Spice [LTSPICE] of the PV module under test. For the simulation of the LIEL measurement under V_{OC} conditions, we simulate the electrical circuit of one PV module under the boundary condition that no external current is flowing. We translate the misalignment of the LIEL hood shown in Fig. 4 a) to partial shading or partial irradiation of some of the cells in the module as shown in Fig. 4 b). Fig. 7 shows the interconnection of the cells in the module and Tab. 1 all used cell parameters. For better conversion of the model we choose to model the cells without a breakdown model. This does not change the simulation results in comparison to a typical cell breakdown voltage of ~-20 V for this module design. The cells are protected by bypass diodes which avoid higher reverse voltage than the cells reverse break through voltage. Each half-cell is simulated by a two-diode model with series and parallel resistance. The cell simulation parameters are chosen in a way that the module datasheet parameters given in Tab. 1 are almost reproduced, when simulating the STC-standard parameter of the used PV module.

Fig. 8 shows the interconnection of the modules with the inverter. For the simulation of the MPP working condition we simulate the two parallel connected strings with 27 PV modules per string at one inverter as the original string setup in the field. The modules are illuminated with sun irradiation ranging from 0 W/m² to 1000 W/m² and the LIEL setup irradiates module side A with an intensity of 1000 W/m² or 2000 W/m². This irradiation range corresponds to a short circuit current of the module of 0.5 and 1 times I_{sc}. In a first step, we search for the MPP working point under the condition of one full module in one of both strings is shaded by the LIEL hood. In a second step we search the current through the side B of the PV module under test at the MPP working conditions. We use the same cell parameters for the MPP simulation as for the V_{OC} simulation.

To compare the electrical circuit simulation and the measured electroluminescence intensity we calculate a proportional value to the electroluminescence intensity ϕ:

$$\phi \sim e^{\frac{eU_d}{k_B T}}, \tag{1}$$

where U_d is the voltage across the half-cell diode, e is the elementary charge, k_B the Boltzmann constant and T the temperature of a half-cell in the PV module. The maximum luminescence intensity ϕ_{max} of the simulation is used to normalize the luminescence intensity ϕ for relative comparisons to measurements.

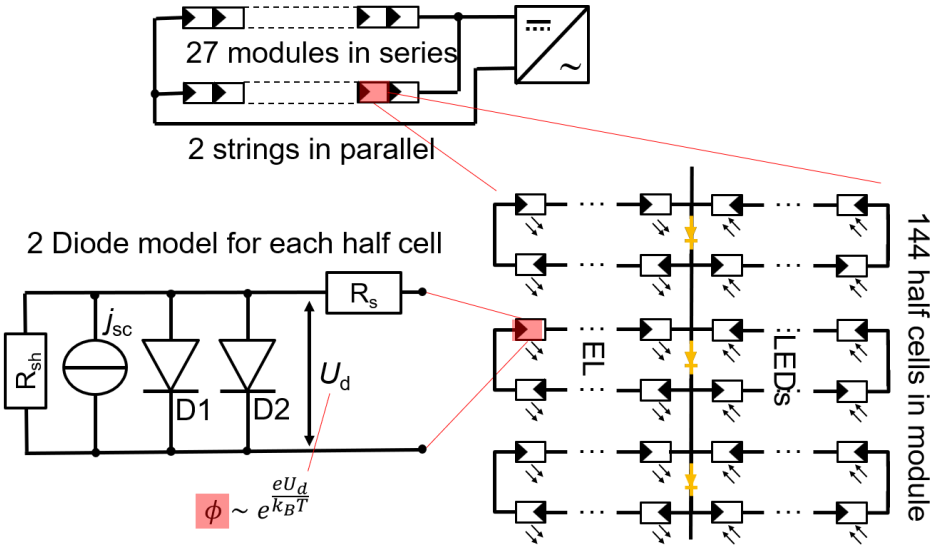

***Figure 7**. The upper part shows the string setup with two parallel strings at one inverter of the tested PV system. One red marked PV module is under LIEL test. Each substring of all modules consists of 24 half-cells. Each cell is simulated by a two-diode model with series R_s and parallel resistance R_{sh}. The diode voltage U_d of the half-cell is used to simulate a value proportional to the electroluminescence intensity ϕ.*

3. Results

Fig. 8 a/b compares two LIEL images with and without dark frame subtraction. The images without dark frame subtraction, Fig. 9a, show a lot stray light form the rear compared to those with dark frame subtraction, Fig. 9b. All following images are therefore taken with dark frame subtraction and only the subtracted images are used for analysis.

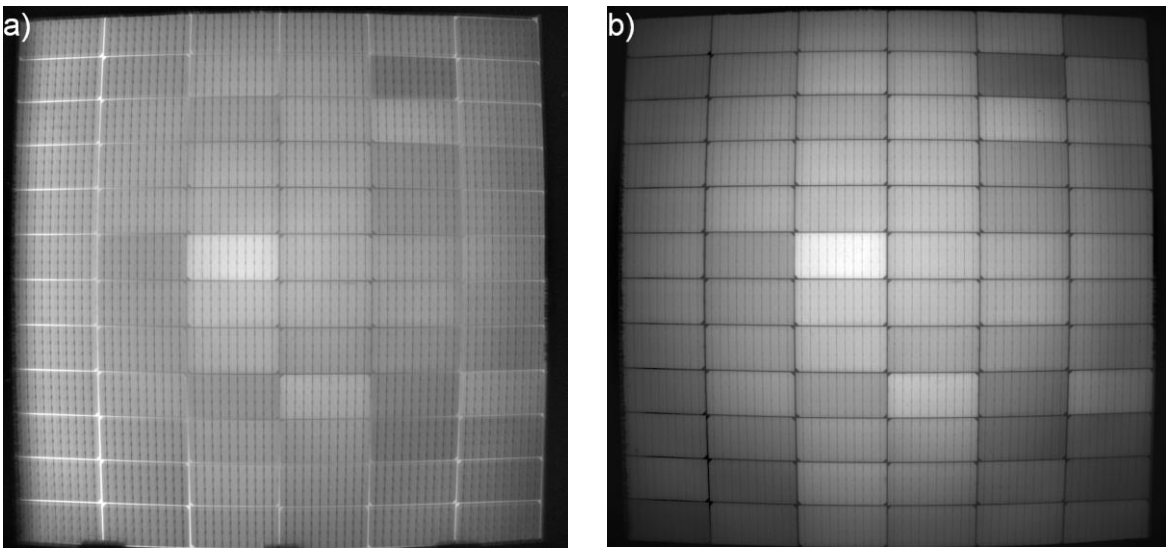

***Figure 8**. LIEL image taken at the MPP operating point, left a) without and right b) with dark frame subtraction. Both images were taken at a solar irradiation of approx. 830 W/m² with an exposure time of 200 ms and optimized for contrast.*

As shown in Fig. 9, LIEL images can be recorded both with module strings separated from the inverter Fig. 9a and with strings tracked by the inverter in the Maximum Power Point (MPP) Fig. 9b. In this example, the images in V_{OC} have a factor of 1.7 higher intensity than the images in MPP. In both cases, the image quality is sufficient for fault analysis. If all modules in a string

show up less EL intensity than other strings the reduced image intensity in Fig. 9b compared to Fig. 9a can be used to differentiate between strings that are connected or not connected to the inverter.

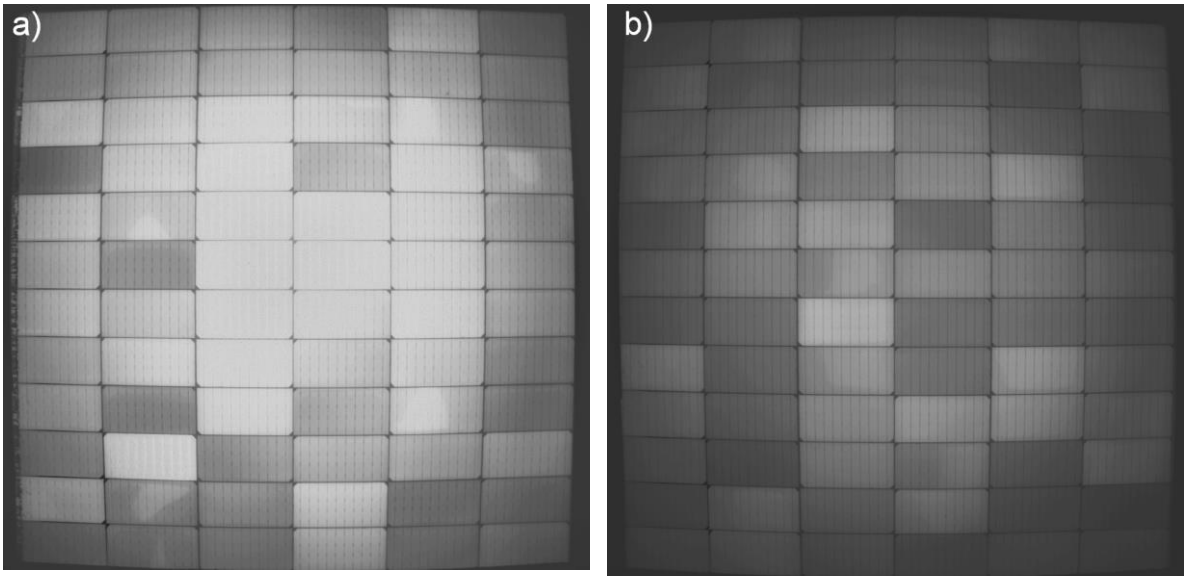

***Figure 9**. LIEL image on the left a) on a PV string in V_{OC} conditions and on the right b) under MPP conditions. Both images were taken at a solar irradiation of 486 W/m² with an exposure time of 200 ms and both are equally increased in intensity and contrast for better visualisation.*

The results of the positioning tests are shown in Fig. 10a and b. The misalignment is measured in units of a half-cell of the module. A misalignment of 1 corresponds to the half-cell width of 92.25 mm incl. cell gap in the string. The direction of the misalignment is defined in Fig. 5. In Fig. 10a LT Spice simulation results are added. In the simulation the edge cells of each string receive only a portion of the light intensity of the string centre cells. The portion is varied between 25% and 100%. The sensitivity of the EL intensity to a misalignment of the LIEL cover on the module increases as the string edge cells receive lower LED irradiation intensity. In Fig. 10b a LT spice simulation is added to the same set of measured EL intensity data. In this case the string edge cells only receive 50% of the LED intensity of the string centre cells. Additionally, the edge cell which peeks out the LIEL cover receives some additional light from the sun. Sun light on the cell peeking out keeps the current through the module on a higher level compared to the case where the peeking cell receives no additional light. Already a small portion of light (250 W/m²) stabilizes the current flow even if one total half-cell (1) peeks for 100% out of the cover. This might be the reason why we measure an EI signal of ~3400 a.u. and ~500 a.u. even if more than one full half-cell peeks out of the cover for 1.1 and 1.2 cells misalignment as the measurements are made at day time. During the misalignment measurement a sun irradiation intensity of 173 W/m² to 246 W/m² was measured in the plane of the PV module array. Please note, that it is not possible to determine the correct sun irradiation on the out-peeking cells as the shade direction of the LIEL cover and the shading due to the handling of the operating staff strongly influence this irradiation intensity and homogeneity on the out-peeking cells.

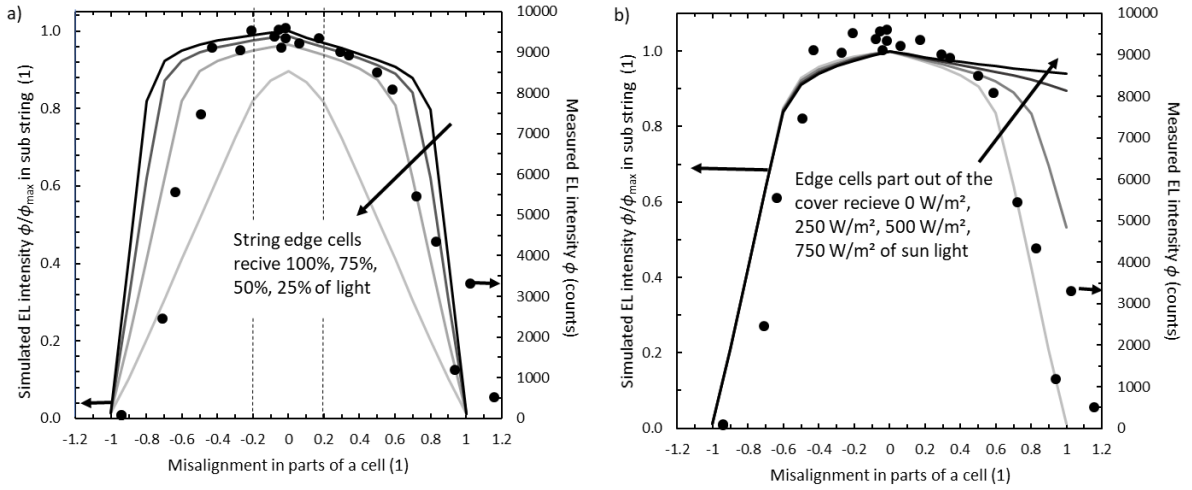

***Figure 10**. In both images a and b, the dots indicate the same measured EL signal intensity as a function of misalignment of the LIEL cover on the module tested under V_{OC} conditions. In plot a) the LT Spice simulation results of the electric current of the luminescing module part is shown with a parameter variation of the LED light intensity at the edge cells relative to the string centre. In plot b) the simulation results of the electric current of the luminescing module part is shown with a parameter variation of sun light intensity at the edge cell that peeks out from under the cover and receives a variation of sun light. In this case the LED illumination on the string edge cells is assumed to be only 50% compared to the string middle cells.*

An evaluation of 261 EL images with regard to the deviation of the LIEL system placement from the target position is shown as a histogram in Fig. 11. It can be seen that 97.7% of all positions are within the tolerance limits of ±18 mm determined above.

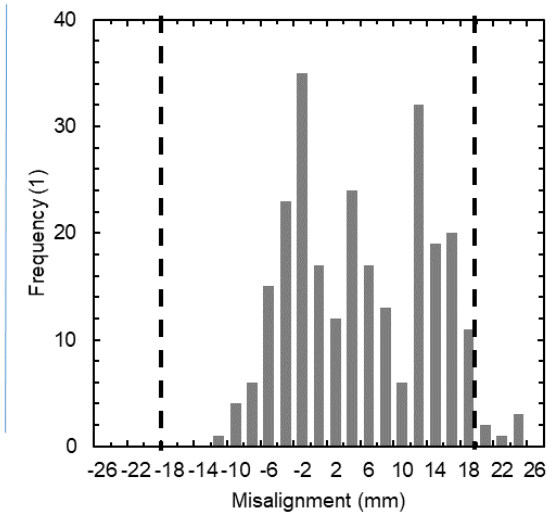

***Figure 11**. Histogram of the misalignment of the LIEL images for 261 recordings in mm.*

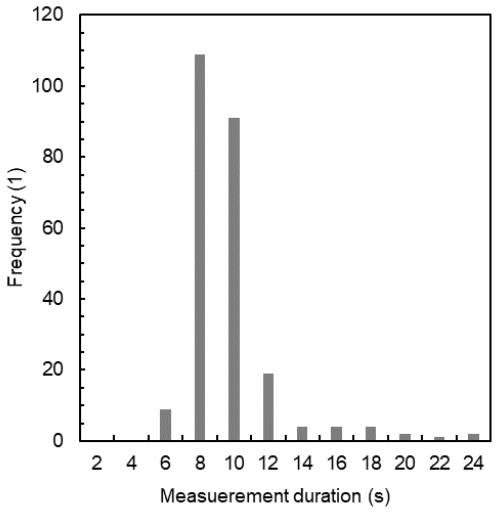

***Figure 12**. Histogram of the measurement duration of the LIEL system in the field incl. hood movement.*

During the field tests we measured also the duration of all measurements incl. the movement of the system from one module to the next. Fig. 12. summarises this data in a histogram. Most measurements last 8 s to 10 s. It is also possible to do the measurement in only 6 s. Due to problems with the prototype control system some of the measurements last substantial longer, up to 24 s.

Fig. 13 shows the influence of the sun irradiation to the luminescence intensity of the LIEL measurement and corresponding simulations of the substring current. The simulation results are shown with the LED intensity as a parameter for 1000 W/m² and 2000 W/m². The experimental and simulation values for 0 W/m² are taken from measurement and simulation values where the inverter is shut down. Measurement and simulation show that the EL intensity and the substring current is decreasing up to 400 W/m² almost linearly with the sun irradiation. The simulation shows for higher sun irradiation a lower slope.

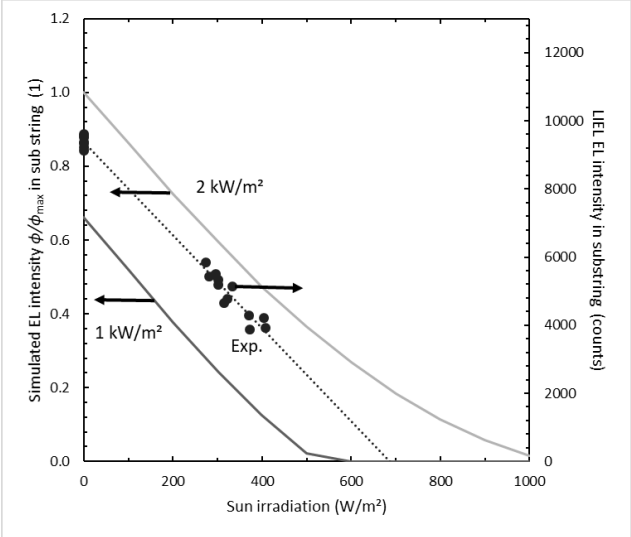

***Figure 13**. Comparison of experimental data of luminescence intensity to simulation results of electric substring current of the module under test as function of the sun irradiation intensity on module level of all other modules in the string. The y-axis is scaled in a way that simulation and experimental data show a similar slope as the proportionality factor between EL counts and substring current is unknown.*

4. Discussion

In the following we discuss the consequences of the LT spice simulation results and the experimental results for the practical application of the LIEL tool in the field. The simulation shows the influence of the positioning, the light inhomogeneity and the sun intensity on the electroluminescence intensity measured with the LIEL system. The inhomogeneity of the LED light at the edge of the cell strings effects the sensitivity of the EL signal intensity to the misalignment of the LIEL cover. Figure 10a shows that the EL signal intensity with well positioned LIEL system is only changed by ~2% even if the string corner cells receive only 50% of the light intensity of the string centre cells. As we see from the measured LED homogeneity of the LIEL system in Fig. 6, the light is inhomogeneous over at least two edge cells at the edge of the LIEL light source. A higher light intensity especially at the edge cells will probably make the LIEL measurement even more robust against displacement of the LIEL tool.

A displacement of the measuring hood of up to ±18 mm (corresponding to 0.2 misalignment in parts of a cell) does not lead to a relevant decrease in the electroluminescence signal for either V_{OC} recordings and is therefore classified as acceptable. ±18 mm is also the thickness of the walls and the separator wall between LED and camera side of the LIEL measurement system. However, one has to keep in mind that a displacement also reduces the view of the camera on one module half. So, a displacement of 18 mm means that 18 mm less of the module half can be seen. This is an additional drawback, but within the 18 mm of tolerance the EL signal intensity of all the other cells does not change more than the reproducibility range of the measurement.

The measurement time for one image of a ready positioned LIEL system is well below 0.5 s. So, the movement of the LIEL system between two measurements has the major impact on the total working speed. In the PV system under test the PV modules are orientated horizontally, compare Fig. 1. That means a double walking distance between two modules (2.279 m) compared to a system with portrait-oriented PV modules (1.134 m). So, these results show the maximum measurement duration. A portrait-oriented PV module in a PV system has half the working distance between the modules and therewith nearly half the measurement duration.

At MPP working conditions the decrease in EL intensity with increasing sun irradiation in Fig. 13 can be explained by examining specific extreme scenarios. When sunlight on the PV modules produces a current higher than what the LEDs of the LIEL system can generate in the tested module, the module's bypass diode goes into reverse voltage bias to carry the larger string current. This results in no EL radiation, as the applied substring voltage is in the wrong direction. If the LED irradiation of the LIEL system causes a slightly higher current on one module half than the MPP current in the rest of the PV string, the bypass diodes does not bypass the string current. In this situation, a basic positive voltage can be achieved, and some EL radiation can be measured. During periods of no sunlight (dark conditions 0 W/m² in Fig. 13), the LIEL system operates unaffected of the inverter, and the LEDs inject the maximum current from the LED side to the electroluminescence side. Under these conditions, we observe the maximum EL signal intensity.

5. Conclusion

The new measurement technology application "light-induced electroluminescence" (LIEL) opens up new possibilities for the inspection of modern PV parks with half-cell modules. The measurement method has many special properties that no other measurement method offers in this combination: the measurement can be carried out in sunlight or at night. It is not necessary to disconnect the electrical connections of the modules. The inverters also do not have to be switched off for the measurement. There are no waiting times for suitable lighting conditions. Depending on the module, a measuring time of 50 ms to max. 200 ms is required for a measurement when using an InGaAs camera. The measurement provides a high-resolution electroluminescence image with 1024 pixels x 2560 pixels of the solar module. The method presented here can even allow to differentiate whether the modules are actively controlled by the inverter or whether modules are not contacted by a difference in EL intensity. The method is robust against incorrect positioning of the measuring hood up to ±18 mm. With the current prototype system, it is possible to record a module including movement to the next module and trigger the next measurement in 12 seconds for both module halves. The movement speed from module to module fully dominates the measurement speed. Subsequent versions will probably be able to drastically reduce this test duration by speeding up the transfer speed of the LIEL hood from module to module. LIEL is a full substitute for pure EL measurements as all features being seen in EL images can also be seen in LIEL images. Only an interrupted interconnect between substrings will make an EL image dark and a LIEL image will not identify this defect or LIEL measurements in mpp condition will recognize an increased image intensity.The new measurement method will make it much easier to find faults in solar modules in solar parks in the future.

Data availability statement

Data used in Fig. 3,5,8-13 are available in [7] under the cc-by licence.

Author contributions

Marc Köntges: Conceptualization, Methodology, Writing - Original Draft, Visualization, Supervision, Funding acquisition

Michael Siebert: Software, Formal analysis, Investigation, Resources, Visualization

Andreas Fladung: Resources, Validation

Jan Schlipf: Writing - Review & Editing, Funding acquisition

Competing interests

The authors declare that they have no competing interests.

Funding

We thank the Federal Ministry of economics and climate actions for funding this work within the LIEL project in the German Central Innovation Programme for SMEs (ZIM) under the funding number KK5291101BS1.

References

1. U. Jahn *et al.*, “Review on Infrared and Electroluminescence Imaging for PV Field Applications,” Report IEA-PVPS T13-10:2018, 2018. [Online accessed 16th Jan. 2022]. Available: http://www.iea-pvps.org/index.php?id=480
2. W. Hermann *et al.*, “Qualification of Photovoltaic (PV) Power Plants using Mobile Test Equipment,” IEA PVPS, Köln, 2021. [Online accessed 16th Jan. 2022]. Available: https://iea-pvps.org/wp-content/uploads/2021/04/IEA-PVPS-T13-24_2021_Qualification-of-PV-Power-Plants_report.pdf
3. Kunz, O., Schlipf, J., Fladung, A., Khoo, Y.S., Bedrich, K.G., Trupke, T., & Hameiri, Z. ,“Outdoor luminescence imaging of field-deployed PV modules,” *Progress in Energy, 4*, 042014, Oct. 2022 doi: 10.1088/2516-1083/ac9a33.
4. M. Vuković *et al.*, “Extraction of photoluminescence with Pearson correlation coefficient from images of field-installed photovoltaic modules,” *J. Appl. Phys.*, vol. 133, no. 21, pp. 76–77, Jun. 2023, doi: 10.1063/5.0151487.
5. G. Alves dos Reis Benatto *et al.*, “Drone-Based Daylight Electroluminescence Imaging of PV Modules,” *IEEE J. Photovoltaics*, vol. 10, no. 3, pp. 872–877, May 2020, doi: 10.1109/JPHOTOV.2020.2978068.
6. M. Köntges, J. Wagner, M. Siebert, S. Bordihn, and C. Schinke, “Applicability of Light Induced Luminescence for Characterization of Internal Series-Parallel Connected Photovoltaic Modules,” *IEEE J. Photovoltaics*, vol. 12, no. 3, pp. 805–814, May 2022, doi: 10.1109/JPHOTOV.2022.3156727.
7. Marc Köntges, Michael Siebert, Andreas Fladung, Jan Schlipf (2024). Dataset: Data for figures in paper "Evaluation of Light-Induced Electroluminescence in PV Field Applications". https://doi.org/10.57702/0qzazwbd